Energy approach to kinetics equations for dislocations and twins and its application for high strain rate collision problems

E N Borodin[1,2] **and A E Mayer**[1]

[1] Chelyabinsk State University, Bratiev Kashirinykh Street 129, Chelyabinsk 454001, Russia
[2] Institute of Problems of Mechanical Engineering of the Russian Academy of Sciences, V.O., Bolshoj pr., 61, Saint Petersburg 199178, Russia

E-mail: elbor7@gmail.com

Abstract. A computational plasticity model with accounting of coupled evolution of the dislocations and twins in metals under the dynamic loading is presented. The model is based on our previous results for the dislocation plasticity, but generalizes them and accounts mechanical twinning in addition. It includes equations of the mechanics of continua for elastic-plastic medium, where the plastic deformation tensor is determined through the structural defects evolution in the material. The model is self-consistent and allows determining of mechanical properties in wide range of strain rates and thermodynamic conditions as well as modification of the defect subsystems. The equations and parameters, its numerical implementation and some of obtained results are presented.

1. Introduction

Constitutive equations are necessary for numerical simulation of materials behaviour in the framework of continuum mechanics. Shear stresses in metals are determined by elastic-plastic properties and plasticity model is a substantial part of the constitutive equations. Experimentally obtainable rates of deformation vary from almost zero (at quasi-static deformation) up to 10^9 s^{-1}—at the thin foils irradiation by the ultra-short laser pulses [1, 2]. Therefore, the plasticity model is greeted to be a wide-range one, which means that it should be valid in a vide range of strain rates as well as in a wide range of thermodynamic parameters. Accounting of structural defects (dislocations and micro-twins) as physical carriers of plasticity is a natural way to construct such a wide-range plasticity model.

Here we present our plasticity model based on the structural defects evolution. Next processes are accounted: motion, generation and immobilization of dislocations [3, 4], formation, growth and immobilization of twins [5]. Interaction of deferent defect subsystems is accounted through their barrier stresses.

Evolution of defect subsystems is described through equations for their concentration (or density) and other characteristics (velocity of dislocations, radius and thickness of twins, for example). It allows one to calculate the plastic strain tensor and the shear stresses—through the generalized Hook's law. Calculation of the structural defects evolution is performed in each physically small volume of metal simultaneously with calculation of its dynamic deformation

on the basis of the continuum mechanics equations. Mechanical response of substance can be calculated in this way as well as the defect subsystems modification [6].

2. Mathematical model—continuum mechanics

Total plastic strain can be represented as a result of the combined action of two competing processes: the dislocation motion and the mechanical twinning. According to this viewpoint, the plastic deformation tensor w_{ik} is represented by the following sum of two tensors: $w_{ik} = w_{ik}^{\mathrm{D}} + w_{ik}^{\mathrm{TW}}$, where w_{ik}^{D} is the part of plastic deformation caused by the dislocation motion, w_{ik}^{TW} is caused by the mechanical twinning. Determination of these tensors through evolution of defect subsystems is considered in the following section.

The common part of the mathematical model consists of three conservation laws. The first one of them is the continuity equation:

$$\frac{1}{\rho}\frac{d\rho}{dt} = -\sum_{k=1}^{N}\frac{\partial v_k}{\partial x_k}, \tag{1}$$

where ρ is the substance density; v_k is velocity vector; x_k is the Cartesian coordinates; N is the number of dimensions of the considered problem, subscript k numerates space directions. The total time derivatives are used in (1) and following equations, which are valid for Lagrangian particles moving with substance. The equation of substance motion:

$$\rho\frac{dv_i}{dt} = -\frac{\partial P}{\partial x_i} + \sum_{k=1}^{N}\frac{\partial S_{ik}}{\partial x_k}, \qquad i = 1, \ldots, N, \tag{2}$$

where P is the pressure or spherical part of stresses, which is determined from a wide-range equation of state $P = P(\rho, U)$ [7–9]; S_{ik} is the tensor of stress deviators, which characterizes the shear stresses; U is the part of internal energy, connected with the spherical part of stresses, its value is determined from the energy conservation law in the following form:

$$\rho\frac{dU}{dt} = \frac{P}{\rho}\frac{d\rho}{dt} + \sum_{i=1}^{N}\sum_{k=1}^{N} S_{ik}\frac{dw_{ik}}{dt}, \tag{3}$$

where the second term in the right-hand part is the heat release due to the plastic strain.

The generalized Hooke law [10] with accounting of the plastic strain w_{ik} is used for determination of the stress deviators:

$$S_{ik} = 2G\left[u_{ik} - \frac{1}{3}\delta_{ik}\sum_{l=1}^{N} u_{ll} - w_{ik}\right], \quad i = 1, \ldots, N, \quad k = 1, \ldots, N, \tag{4}$$

where $G = G(T, P)$ is the shear modulus, which depends on temperature and pressure [11]; δ_{ik} is the bivalent mixed tensor; u_{ik} is the geometrical deformation, induced by the macroscopic motion of substance, which is determined by the following equation:

$$\frac{du_{ik}}{dt} = \frac{1}{2}\left[\frac{\partial v_i}{\partial x_k} + \frac{\partial v_k}{\partial x_i}\right] + \frac{1}{2}\sum_{l=1}^{N}\left\{u_{il}\left(\frac{\partial v_k}{\partial x_l} - \frac{\partial v_l}{\partial x_k}\right) + u_{lk}\left(\frac{\partial v_i}{\partial x_l} - \frac{\partial v_l}{\partial x_i}\right)\right\}, \tag{5}$$

where the first term in the right-hand part is the infinitesimal strain rate tensor; the second term accounts for the change of the geometrical deformation tensor components in the laboratory coordinate system due to the substance rotation [12], which is essential for two- or three-dimensional cases.

3. Mathematical model—evolution of structural defects

Two main types of structural defects—dislocations and micro-twins are considered here together with their contributions in the total plastic strain. Contribution of twinning can be zero $w_{ik}^{\mathrm{TW}} = 0$ for metals with the suppressed twinning, aluminum for example. In the common case, both parts are taken into account.

Submodels of the dislocation plasticity and the mechanical twinning consist of kinetics equations for defects ensembles and equations for corresponding contributions, w_{ik}^{D} and w_{ik}^{TW}, in the total plastic strain. Dislocations are characterized by scalar densities of mobile and immobilized dislocations and velocity of mobile dislocations; these quantities are determined for each possible slip system of dislocations in the considered metal and for each physically small volume of substance. Thus, we use the continuum theory of dislocations. Twins are supposed to be cylindrical and characterized by concentrations of mobile and immobilized twins (with fixed boundaries), their radii and thicknesses. All possible crystallographic orientations of twins are also taken into account.

3.1. Dislocations

The plastic deformation tensor of the dislocation plasticity w_{ik}^{D} can be found from the generalized Orowan equation [13]:

$$\frac{dw_{ik}^{\mathrm{D}}}{dt} = \sum_{\beta} \frac{1}{2}\left(b_i^{\beta} n_k^{\beta} + b_k^{\beta} n_i^{\beta}\right) V_{\mathrm{D}}^{\beta} \rho_{\mathrm{D}}^{\beta} + \frac{1}{2}\sum_{l=1}^{N}\left\{ w_{il}^{\mathrm{D}}\left(\frac{\partial v_k}{\partial x_l} - \frac{\partial v_l}{\partial x_k}\right) + w_{lk}^{\mathrm{D}}\left(\frac{\partial v_i}{\partial x_l} - \frac{\partial v_l}{\partial x_i}\right)\right\}, \quad (6)$$

where the first term in the right-hand part is the plastic strain rate itself while the second term accounts for the rotation of the substance elements, like in (5). Superscript β numerates the slip systems of dislocations in the material, which are characterized by the Burgers vector b_i^{β} and by the normal n_i^{β} to the slip plane; $\rho_{\mathrm{D}}^{\beta}$ is the scalar density of mobile dislocations in the corresponding slip system; V_{D}^{β} is velocity of these dislocations relative to the substance.

One has to take into account the different crystallographic orientations of lattice in different grains for description of the polycrystalline metals. Simulations [3] had shown that the most suitable oriented slip planes are activated first of all. Therefore, it is enough to account only such "active" planes, which orientations are close throughout the sample, regardless of the grain boundaries. This is very handy approximation, especially for the nanocristalline metals, where the grains are much smaller than the numerical grid resolution.

The core of the dislocation plasticity model [3,4] consists of the motion and kinetics equations. The equation of dislocations motion is the following:

$$m_0 \xi_{\beta}^3 \frac{\mathrm{d}V_{\mathrm{D}}^{\beta}}{\mathrm{d}t} = \left[\sum_{i=1}^{N}\sum_{k=1}^{N} S_{ik} b_i^{\beta} n_k^{\beta} \pm \frac{1}{2} bY\right] - B\xi_{\beta}^3 V_{\mathrm{D}}^{\beta}, \quad (7)$$

where $\xi_{\beta} = 1/\sqrt{1 - \left(V_D^{\beta}/c_{\mathrm{t}}\right)^2}$ is a quasi-relativistic factor [14], which reflects the restriction that $\left|V_D^{\beta}\right| < c_{\mathrm{t}}$; $c_{\mathrm{t}} = \sqrt{G/\rho}$ is the transverse sound speed of the material; $m_0 \approx 10^{-16}$ kg/m is the rest mass of dislocations; Y is the static yield strength; B is the phonon drag coefficient, it describes the viscous resistance to the dislocation motion [15]. Dislocations move only if the force of the shear stresses (the first term in the square brackets in Eq.(7)) is higher than the resistance of the Peierls relief, inclusions and other defects, which is $bY/2$; the sign "$\pm$" means that the resistance is always directed opposite to the dislocation motion.

The kinetics equations for mobile $\rho_{\mathrm{D}}^{\beta}$ and immobilized $\rho_{\mathrm{I}}^{\beta}$ dislocations are [4]:

$$\frac{\mathrm{d}\rho_{\mathrm{D}}^{\beta}}{\mathrm{d}t} = Q_{\mathrm{D}}^{\beta} - Q_{\mathrm{I}}^{\beta} - Q_{\mathrm{Da}}^{\beta}, \frac{\mathrm{d}\rho_{\mathrm{I}}^{\beta}}{\mathrm{d}t} = Q_{\mathrm{I}}^{\beta} - Q_{\mathrm{Ia}}^{\beta}, \tag{8}$$

where Q_{D}^{β} is the generation rate of the mobile dislocations; Q_{I}^{β} is the rate of immobilization; Q_{Da}^{β} and Q_{Ia}^{β} are the annihilation rates of the mobile and immobilized dislocations respectively:

$$Q_{\mathrm{Da}}^{\beta} = k_{\mathrm{a}} b \left|V_{\mathrm{D}}^{\beta}\right| \rho_{\mathrm{D}}^{\beta} \left(2\rho_{\mathrm{D}}^{\beta} + \rho_{\mathrm{I}}^{\beta}\right) - \left|V_{\mathrm{D}}^{\beta}\right| \rho_{\mathrm{D}}^{\beta}/d, \quad Q_{\mathrm{Ia}}^{\beta} = k_{\mathrm{a}} b \left|V_{\mathrm{D}}^{\beta}\right| \rho_{\mathrm{D}}^{\beta} \rho_{\mathrm{I}}^{\beta}, \tag{9}$$

where k_a is the annihilation factor; d is the grain diameter in polycrystals; b is the modulus of Burgers vector of dislocations. Rates of generation and immobilization are as follows:

$$Q_{\mathrm{D}}^{\beta} = \frac{0.1}{\varepsilon_{\mathrm{D}}} \left\{2\, B\, c_{\mathrm{t}}^{2}\ [\xi_{\beta} - 1] + b\, Y\ \left|V_{\mathrm{D}}^{\beta}\right|\right\}\ \rho_{\mathrm{D}}^{\beta}, \tag{10}$$

$$Q_{\mathrm{I}}^{\beta} = V_{\mathrm{I}} \left(\rho_{\mathrm{D}}^{\beta} - \rho_0\right) \sqrt{\rho_{\mathrm{I}}^{\beta}}, \tag{11}$$

where $\varepsilon_{\mathrm{D}} \approx 8$ eV$/b$ is the energy of the dislocations formation per unit length. The multiplier in curly brackets in (10) is the energy dissipation rate per unit length of dislocation—it is the sum of work against the phonon friction and the work against the resistance force [14]. Equation (11) describes the immobilization process, where parameter $\rho_0 \approx 10^7$ cm^{-2} is the minimal dislocation density, which is necessary for their consolidation in the structures [4]. This expression is written from the assumption that all excess mobile dislocations will be immobilized in structures with the characteristic time $\tau_I^{\beta} \approx r_I^{\beta}/V_I$, where $r_I^{\beta} \approx \left(\rho_I^{\beta}\right)^{-1/2}$ is the average distance between the immobile dislocations. Parameter V_I means a characteristic velocity of the dislocations movement during the process of consolidation; it is determined by internal stresses.

The drag coefficient B depends on the temperature [16]:

$$B = T\ \left(4\theta^2 k_{\mathrm{B}}^3\right) / \left(h^2 c_{\mathrm{b}}^3\right), \tag{12}$$

where k_B is the Boltzmann constant; h is the Planck constant; θ is the parameter with the dimensionality of temperature; c_{b} is the bulk sound velocity. The static yield strength is determined by the relation:

$$Y = Y_0 + AGb\sqrt{\rho_{\mathrm{I}}} + k_{\mathrm{HP}}/\sqrt{d} + k_{\mathrm{TW}}/\sqrt{\Delta}, \tag{13}$$

where ρ_{I} is the total scalar density of immobilized dislocations (the sum over all slip planes); Δ is an average distance between the twins; A is the interaction constant of dislocations, k_{HP} is the Hall-Petch constant and k_{TW} is similar constant for twins. In the right-hand part of equation (13): Y_0 is the resistance of Peierls relief and point defects (inclusions); the second term is resistance of immobile dislocations (Taylor law), the third term is contribution of grain boundaries (Hall-Petch law) and the last term expresses the resistance of twins in a similar way to the grain boundaries [5].

Parameters of the dislocation plasticity model have been found in [4] by comparison with velocity histories of back surface at plate impact tests.

3.2. Twins

Twinning becomes an alternative plasticity mechanism at low temperatures and high strain rates [17, 18]. The stacking fault energy γ_{SF} is the main parameter determining the material tendency to undergo the twinning. Metals with low stacking fault energy (less than $100\,\mathrm{mJ/m^2}$), such as various grades of steel, copper, silver, nickel and their alloys, are disposed to twinning.

The plastic deformation caused by twins can be expressed through its volume fraction:

$$\frac{dw_{ik}^{\mathrm{TW}}}{dt} = \sum_{\gamma} \frac{d\alpha^{\gamma}}{dt} \left(\tau_i^{\gamma} n_k^{\gamma} + \tau_k^{\gamma} n_i^{\gamma}\right) \varepsilon_{\mathrm{TW}} + \frac{1}{2} \sum_{l=1}^{N} \left\{ w_{il}^{\mathrm{TW}} \left(\frac{\partial v_k}{\partial x_l} - \frac{\partial v_l}{\partial x_k}\right) + w_{lk}^{\mathrm{TW}} \left(\frac{\partial v_i}{\partial x_l} - \frac{\partial v_l}{\partial x_i}\right) \right\}, \tag{14}$$

where α^{γ} is the volume fraction of twinned material; $\varepsilon_{\mathrm{TW}}$ is the deformation of twinned material with respect to initial one, for example $\varepsilon_{\mathrm{TW}} = 1/\sqrt{2}$ in fcc and bcc metals [18]; unit vectors τ_k^{γ} and n_k^{γ} describes crystallographic orientation of twins; superscript γ numerates all possible orientations. The second term in the right-hand part plays the same role as in (5) and (6).

We suppose that twins are cylindrical and have the same radius and thickness in a physically small substance element, than the volume fraction is equal to

$$\alpha^{\gamma} = N_{\mathrm{TW}}^{\gamma} \left(\pi \left(R_{\mathrm{TW}}^{\gamma}\right)^2 h_{\mathrm{TW}}^{\gamma}\right) + N_{\mathrm{IM}}^{\gamma} \left(\pi \left(R_{\mathrm{IM}}^{\gamma}\right)^2 h_{\mathrm{IM}}^{\gamma}\right), \tag{15}$$

where N_{TW}^{γ} and N_{IM}^{γ} are the local concentrations of twins, mobile and immobilized respectively; R_{TW}^{γ} and R_{IM}^{γ} are the radii of mobile and immobilized twins; h_{TW}^{γ} and h_{IM}^{γ} are their thicknesses. All these values are determined by the kinetics of twins.

Energy of a twin consists of the surface part determined by the stacking fault energy, the energy in external stresses and the energy of elastic deformations of the surrounding matrix [19]. Differentiation of this energy over radius or thickness gives the forces tending to change the corresponding size of the twin:

$$F_R^{\gamma} = 4\pi\varepsilon_{\mathrm{TW}} R_{\mathrm{TW}}^{\gamma} h_{\mathrm{TW}}^{\gamma} \sum_{k=1}^{N} \sum_{i=1}^{N} S_{ik} n_i^{\gamma} \tau_k^{\gamma} - 2\pi\gamma_{\mathrm{SF}} \left(2R_{\mathrm{TW}}^{\gamma} + h_{\mathrm{TW}}^{\gamma}\right) - \Phi \left(h_{\mathrm{TW}}^{\gamma}\right)^2, \tag{16}$$

$$F_h^{\gamma} = 2\pi\varepsilon_{\mathrm{TW}} \left(R_{\mathrm{TW}}^{\gamma}\right)^2 \sum_{k=1}^{N} \sum_{i=1}^{N} S_{ik} n_i^{\gamma} \tau_k^{\gamma} - 2\pi\gamma_{\mathrm{SF}} R_{\mathrm{TW}}^{\gamma} - 2\Phi R_{\mathrm{TW}}^{\gamma} h_{\mathrm{TW}}^{\gamma}, \tag{17}$$

where $\Phi = 2\pi^3 (2-\nu) / [3(1-\nu)] G\varepsilon_{\mathrm{TW}}^2$, ν is the Poisson ratio. Growth of twin radius or thickness is connected with motion of twinning dislocations at its edges, which are the partial dislocations. The balance between the described above forces (expressions (16) and (17)) and the drag force acting on these dislocations allows one to find the growth equations:

$$\dot{R}_{TW}^{\gamma} \left(1 - (\dot{R}_{TW}^{\gamma}/c_t)^2\right)^{-3/2} = b F_R^{\gamma} \left[2\pi R_{TW}^{\gamma} h_{TW}^{\gamma} B^{part}\right]^{-1}, \tag{18}$$

$$\dot{h}_{TW}^{\gamma} \left(1 - \left(R_{TW}^{\gamma} \dot{h}_{TW}\right)^2 / (bc_t)^2\right)^{-3/2} = b F_h^{\gamma} \left[\pi \left(R_{TW}^{\gamma}\right)^2 B^{part}\right]^{-1}, \tag{19}$$

where $B^{part} \approx B/3$ is the drag coefficient of partial dislocations.

Equations (16)–(19) give the critical radius $R^{\gamma}_{\rm cr}$ and the thickness $h^{\gamma}_{\rm cr}$ of twin at which forces are equal to zero—a twin larger than the critical one will grow up. Immobilized twins can not grow in radius but they can change its thickness similar to equations (17), (19).

A twin can growth in the external stress field if its radius and thickness are larger than the critical sizes R^{γ}_0 and h^{γ}_0, at which $F^{\gamma}_R = 0$:

$$R^{\gamma}_0 = \frac{\gamma_{SF}}{K} + \frac{\Phi}{\pi K} h^{\gamma}_0, \quad h^{\gamma}_0 = 0.5\left(\sqrt{L^2 + 4M} - L\right), \tag{20}$$

$$K = \varepsilon_{TW} \sum_{k=1}^{N}\sum_{i=1}^{N} S_{ik} n^{\gamma}_i \tau^{\gamma}_k, \quad L = \frac{4\pi\gamma^2_{SF}}{3\Phi}\left(1 - \frac{2\Phi}{\pi K}\right), \quad M = \frac{4\pi\gamma^2_{SF}}{3\Phi K}. \tag{21}$$

Smaller twins collapse as the force $F^{\gamma}_R < 0$, in this case. Estimation shows that $h^{\gamma}_0 > 3b$ in the conditions typical for twinning at the shock-wave loading.

The last part of the twinning model is the kinetics equations for concentrations of twins. We have written them from energetic consideration supposing that the twinning becomes an active channel of plastic strain then the dislocation plasticity becomes ineffective. Twins are experimentally observed usually then the dislocation plasticity is suppressed. Effectiveness of the dislocation channel is restricted by annihilation of dislocations (see (9)). A part of plastically dissipated energy spends on formation of new defects [20, 21], but in conditions of active annihilation this energy can not be stored in the dislocation subsystem and should be stored in other types of defects, twins for example. Thus, the generation rate of twins

$$\dot{N}^{\gamma+}_{\rm TW} = \varepsilon_{\rm D}\, Q_a / \left(4\pi (R^{\gamma}_{\rm cr})^2 \gamma_{\rm SF}\, \gamma_0\right), \tag{22}$$

where $Q_a = \sum_{\beta}\left(Q^{\beta}_{\rm Da} + Q^{\beta}_{\rm Ia}\right)$ is the total annihilation rate of dislocations; γ_0 is the total number of possible orientations of twins. A twin becomes immobilized then it reaches a grain boundary or another twin; the immobilization rate can be written as follows:

$$\dot{N}^{\gamma-}_{\rm TW} = N^{\gamma}_{\rm TW} \left| dR^{\gamma}_{\rm TW}/dt \right| \left(\Delta^{-1} + d^{-1}\right), \tag{23}$$

The average distance between the twins Δ is connected with their volume fraction [17] $\Delta^{-1} = \sum_{\gamma}\left[\alpha^{\gamma} / \left\{(1-\alpha^{\gamma})\, h^{\gamma}_{\rm TW}\right\}\right]$. Finally, the required kinetics equations are the following:

$$\frac{dN^{\gamma}_{\rm TW}}{dt} = \dot{N}^{\gamma+}_{\rm TW} - \dot{N}^{\gamma-}_{\rm TW}, \quad \frac{dN^{\gamma}_{\rm I}}{dt} = \dot{N}^{\gamma-}_{\rm TW}. \tag{24}$$

In spite of seeming complexity, the twinning model requires only one additional parameter, the stacking fault energy γ_{SF}; all other parameters are defined in the frames of the dislocation plasticity model [4]. For copper we use $\gamma_{\rm SF} = 45$ mJ/m^2. Implementation of this twinning model to the plate impact tests gives results corresponding to the experimental observations as it had been shown in [5].

4. Numerical implementation

The described above plasticity model is numerically realized in CRS computer program in 1D and 2D cases [22]. This program is designed to simulate various intensive actions on metal: high-speed impact, intensive electron, ion and laser irradiation.

Method of separation by physical processes is used with the following subproblems: i) substance dynamics ((1)–(3)) dislocations kinetics and motion; iii) twinning. Equations for

all these processes are solved independently on each time step, and the data exchange takes place at the end of each step. Subproblem of the substance dynamics are solved by modification of the numerical method [23]. Modification consists in eliminating of the artificial viscosity and accounting of the physical viscosity; it allows one to obtain the stable numerical solution by using of a fine enough computational grid [24]. Equation (7) for the dislocation velocity is solved using the approximate analytical solution [14]. All other equations are solved by Euler method with a varied time step.

5. Calculation results

In this section we present some results obtained with use of the described above plasticity model with the kinetics of structural defects.

5.1. Strain rate dependence of the dynamic yield strength

Figure 1 presents the calculated strain rate dependences of the maximum shear stress in the coarse grained copper (the limit $d \to \infty$) with varied initial dislocation densities in comparison with the experimental and calculated data taken in its adapted form from [25]. A uniaxial compression of a small substance volume had been simulated with the constant strain rate $\partial v/\partial z = \dot{\varepsilon}$ to obtain each point of these dependences.

The presented in figure 1 maximal shear stress is equal to the one half of the dynamical yield strength. The experimental and calculated dependences have two distinct regions: at the low and moderate strain rates the dynamic yield strength increases slowly with the strain rate—the regime of dislocation velocity control according to [25], while after some point the shear stress growth becomes very sharp—the regime of dislocation generation control [25]. This sharp growth of shear strength is a manifestation of the dislocation starvation, and the used dislocation plasticity model can uniformly describe both regimes. According to obtained results, the different strain rate dependences ascertained in [25] can be explained by different initial densities of structural defects (dislocations) in the loaded material. Increase of initial defects concentration leads to decrease of the shear strength at high strain rates $> 10^6$ s^{-1}.

5.2. Localization of plastic flow on the shock front

The proposed model has been used for numerical investigation of the plastic flow localization [26]. Figure 2 shows the picture of the plastic flow localization behind the shock wave front. The shock wave moves through a sample with the randomly perturbed dislocation density. One can see formation of the shear bands inclined on 45 degrees to the shock wave front. The similar results have been obtained for perturbation of grain size; any investigated perturbation leads to nonuniformity.

5.3. Structure evolution due to Taylor anvil-on-rod impact test

Modeling of the process of Taylor anvil on rod compaction of copper samples at various impact velocities (from 88 m/s up to 500 m/s) was performed. In calculations, anvil is modeled as a rigid plane obstacle with free sliding of the rod material along this plane; initial velocity field is uniform within the rod and directed toward the anvil. Taking into account, separately or simultaneously, both mechanisms of plasticity, the slipping of dislocation and the twinning, allows one to investigate contributions of these mechanisms in the total plastic deformation and to analyze their influence on formation of the complex rod shape after compaction. Profiles of copper rod (with initial 75 mm length and 19 mm diameter) in the process of compaction are presented in figure 3 for relatively low (a) and high (b) initial velocities of the rod. In these calculations, the twinning is not taken into account.

Figure 3 shows that the evolution of the dislocation subsystem is inhomogeneous by volume of material. At relatively low strain rate, dislocation density grows up inside the individual bands.

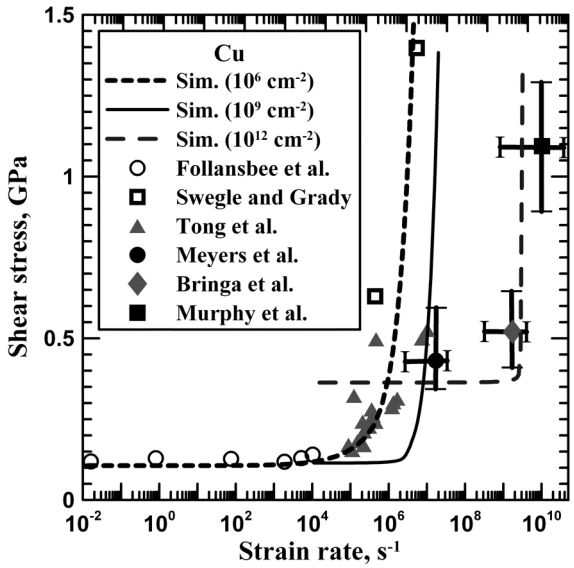

Figure 1. Strain rate dependences of maximal shear stress (the dynamical yield strength) for coarse-grained copper. Markers are experimental and calculated (MD) results of different authors taken from [25]. Lines present our simulation results for various initial dislocation densities. Scattering of experimental points at large strain rates can be explained by difference of the initial dislocation density of samples.

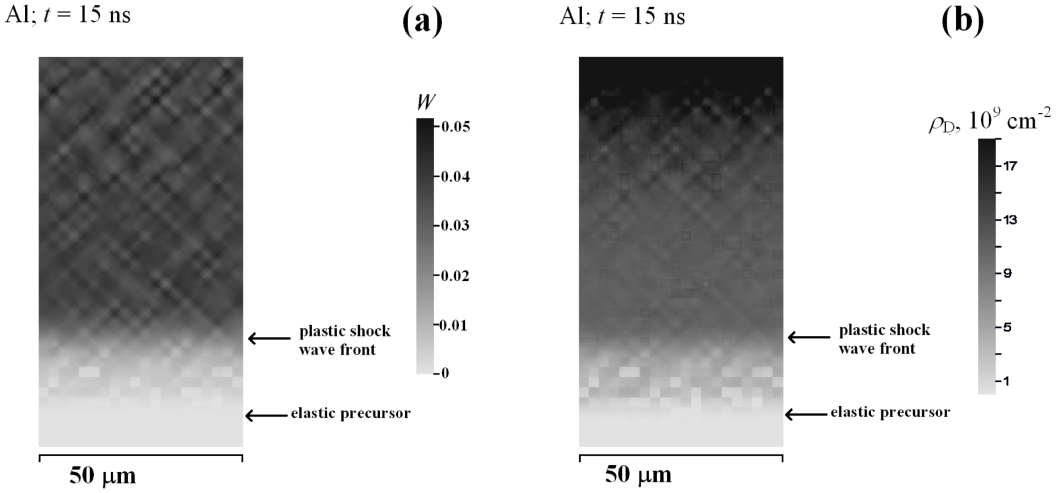

Figure 2. Localization of plastic flow on the shock wave front: the shock wave propagation in aluminium with the randomly perturbed initial distribution of dislocation density; the plastic strain intensity (a) and the dislocation density (b). Formation of shear bands inclined on 45 degrees to the shock wave front is observed. Velocity jump in the shock wave is 0.3 km/s, it moves downwards.

With the increasing of deformation degree, the number of bans also increases and distribution of the dislocation density in the sample became almost homogeneous. Another picture one can see at high strain rate (more than 200 m/s)—against the background of homogeneous dislocation density, the macroscopic shear bands grow towards the shock wave propagation. One can see

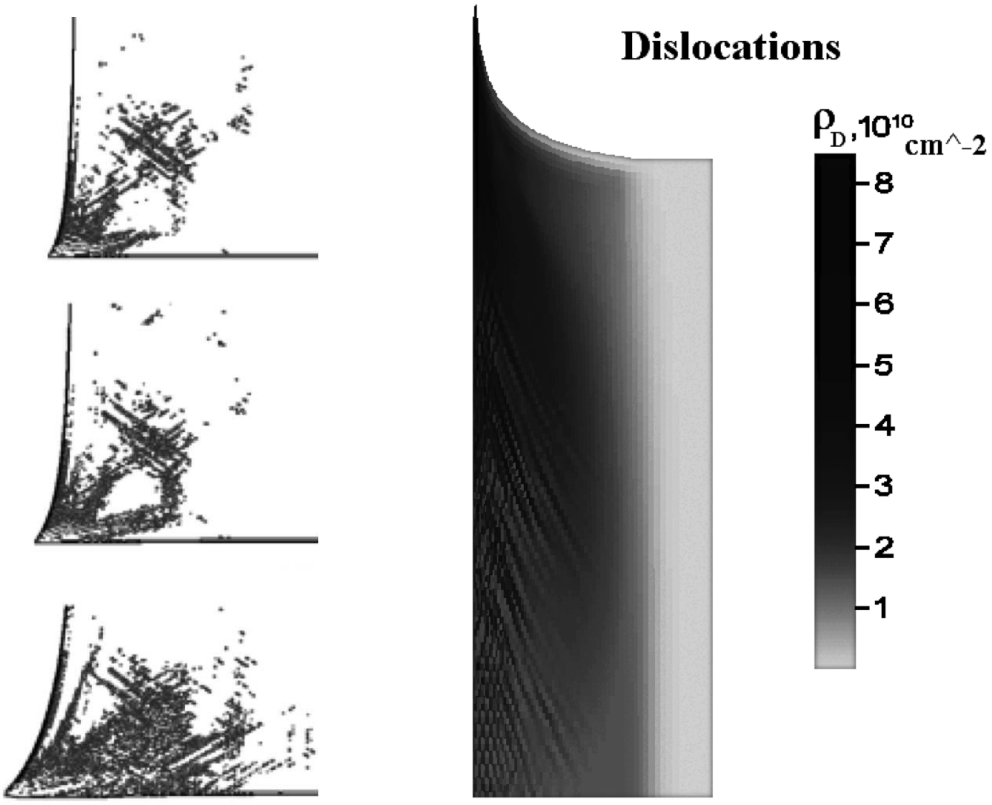

Figure 3. Profile of copper rod (with initial length of 75 mm and diameter of 19 mm) in the process of compaction and distribution of dislocations for relatively low (<100 m/s) (a) and high (>300 m/s) (b) initial velocities of the rod.

the localization of the plastic deformation behind the shock wave in the form of inclined shear bands with increased density of dislocations similar to that reported in [27, 28].

Calculations with accounting of twinning also were done. Spatial distribution of twins is also nonuniform and has a tendency to macroscopic localization determined by the geometry of the problem, as well as microscopic localization on much smaller scale. Qualitatively, this distribution has a very good agreement with the calculation [29] made on the basis of an empirical model of twinning. An intensive flattening on the level of colliding base that is typical to the case of dislocation plasticity (see figure 3) combines with a wide zone of deformation. Both the dislocation plasticity and twinning make substantial contributions in total plastic deformation of the rod. In the first stage of collision, the twinning plays the major role; the action of twining creates a wide zone of plastic deformation near the base (figure 4). Further, the process of dislocation plasticity begins in the twinned part of the sample, which leads to the observed flattening of the base. It is interesting to note that the degree of homogeneity of the twin distribution changes with the increasing initial speed of the rod. At relatively low (100 m/s, see figure 4(a)) and high speeds (300 m/s, see figure 4(b)), the distribution of twins is almost uniform near the base of the rode, while at intermediate speeds (200 m/s, see figure 4(c)) one can clearly distinguish two twinned regions—near the lower corner of the rod, where there are highest plastic deformation degree, and near the axis of the rod.

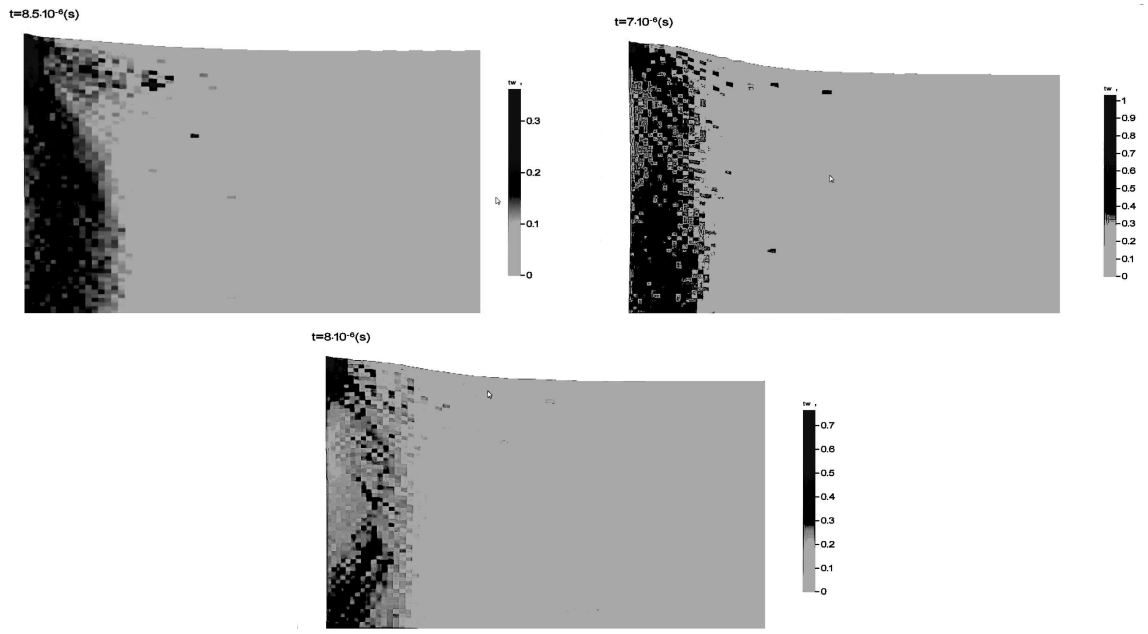

Figure 4. Taylor anvil-on-rod impact test. Distribution of twins in the rod at 8.5 microseconds with impact velocity of 100 m/s (a), at 7 microseconds with impact velocity of 300 m/s (b) and at 8 microseconds with impact velocity of 200 m/s (c).

6. Conclusions

Description of the dynamics and kinetics of structural defects is a natural way to take into account the inertness of plastic relaxation. This approach can be used for construction of a wide-range plasticity model as an important element of the constitutive equations for the continuum mechanics modelling.

Here we present the plasticity model which simultaneously takes into account the dislocations gliding and mechanical twinning as competing plasticity mechanisms. Results of calculations with the use of the model are in accordance with the experimental data. The model can be developed by accounting of additional physical processes.

The original approach for energy distribution due to plastic deformation allows us to propose a new model for mechanical twinning as a natural extension of the dislocation plasticity model. The proposed approach allows one to calculate the modification of defects subsystems and the correlated mechanical properties during the dynamic loading.

At high strain rates $> 10^6$ s^{-1}, the inertness of plasticity plays the critical role: the shear strength strongly depends on the initial concentration of defects. Increase of the initial dislocation density leads to the decrease of the shear strength at such conditions.

Our approach allows one to investigate the localization of plastic flow and heterogeneity of defect structure distribution behind the shock wave front.

Acknowledgments

This study was supported by grants of the President of the Russian Federation (MD-286.2014.1), the Russian Foundation for Basic Research (12-02-31375, 14-01-00814) and the Ministry of Education and Science of the Russian Federation (State Task of Chelyabinsk State University No. 3.1334.2014/K).

References

[1] Whitley V H, McGrane S D, Eakins D E, Bolme T A, Moore D S and Bingert J F 2011 *J. Appl. Phys.* **109** 013505
[2] Inogamov N A, Zhakhovsky V V, Petrov Y V, Khokhlov V A, Ashitkov S I, Khishchenko K V, Migdal K P, Ilnitsky D K, Emirov Y N, Komarov P S, Shepelev V V, Miller C W, Oleynik I I, Agranat M B, Andriyash A V, Anisimov S I and Fortov V E 2013 *Contrib. Plasma. Phys.* **53** 796–810
[3] Krasnikov V S, Mayer A E and Yalovets A P 2011 *Int. J. Plast.* **27** 1294–1308
[4] Mayer A E, Khishchenko K V, Levashov P R and Mayer P N 2013 *J. Appl. Phys.* **113** 193508
[5] Borodin E N, Atroshenko S A and Mayer A E 2014 *Techn. Phys.* **59** 1163–1170
[6] Krasnikov V S and Mayer A E 2012 *Surf. Coat. Techn.* **212** 79–87
[7] Kolgatin S N and Khachatur'yants A V 1982 *Teplofiz. Vys. Temp.* **20** 90–94
[8] Fortov V E, Khishchenko K V, Levashov P R and Lomonosov I V 1998 *Nucl. Instr. Meth. Phys. Res. A* **415** 604–608
[9] Khishchenko K V 2015 *J. Phys.: Conf. Series* This issue (*Preprint* `arXiv:1510.00763`)
[10] Landau L D and Lifshitz E M 1986 *Course of Theoretical Physics, Vol. 7.* (Oxford: Butterworth-Heinemann)
[11] Guinan M W and Steinberg D J 1974 *J. Phys. Chem. Solids* **35** 1501–1512
[12] Wilkins M L 1963 Calculation of elastic-plastic flow Report UCRL-7322
[13] Kosevich A M 1965 *Sov. Phys. Uspekhi* **7** 837–854
[14] Dudorov A E and Mayer A E 2011 *Vestn. Chelyab. State Univ. Phys.* **39** 48–56
[15] Alshitz V A and Indenbom V L 1975 *Sov. Phys. Uspekhi* **18** 1–20
[16] Suzuki T, Takeuchi S and Yoshinaga H 1991 *Dislocation Dynamics and Plasticity* (Berlin: Springer)
[17] Allain S, Chateau J P and Bouaziz O A 2004 *Mater. Sci. Eng. A* **387-389** 143–147
[18] Christian J W and Mahajan S 1995 *Prog. Mat. Sci.* **39** 1–157
[19] Eshelby J 2007 *The determination of the elastic field of an ellipsoidal inclusion and related problems. Collected works of J D Eshelby* (Springer)
[20] Kittel C 2004 *Introduction to Solid State Physics* (New York: Wiley)
[21] Plekhov O A, Naimark O B, Saintier N and Palin-Luc T 2009 *Tech. Phys.* **54** 1141–1146
[22] Mayer A E, Borodin E N, Krasnikov V S and Mayer P N 2014 *J. Phys.: Conf. Series* **552** 012002
[23] Yalovets A 1997 *J. Appl. Mech. Tech. Phys.* **38** 137–150
[24] Mayer A E and Khishchenko K V 2014 *Physics of Extreme States of Matter—2014* (Chernogolovka: IPCP RAS) pp 45–48
[25] Armstrong R and Zerilli F J 2010 *J. Phys. D: Appl. Phys.* **43** 492002
[26] Mayer A, Borodin E N and Mayer P N 2013 *J. Phys. D: Appl. Phys.* **51** 188–199
[27] Borodin E N and Mayer A E 2013 *Tech. Phys.* **58** 1159–1163
[28] Krasnikov V S and Mayer A E 2014 *Mater. Sci. Eng. A* **619** 354–363
[29] Lapczyk I, Rajagopal K R and Srinivasa A R 1998 *Computational Mechanics* **21** 20–27